


RESEARCH

Open Access



DMC-BH derivative DMC-GF inhibits the growth of glioma stem cells by targeting the TRIM33/SLC25A1/mitochondrial oxidative phosphorylation pathway

Lei Shi^{1†}, Xifeng Fei^{2†}, Jian Huang^{3†}, Bao He^{1†}, Zhixiang Sun^{1†} and Guan Sun^{4*} 

Abstract

Glioma stem cells (GSCs) exhibit significant resistance to conventional radiotherapy and chemotherapy, contributing to high recurrence rates in gliomas. Addressing this critical clinical need, we developed DMC-GF, a novel GLUT1-based curcumin derivative, to enhance brain specificity and metabolic stability compared to its predecessor DMC-BH. Pharmacokinetic studies in rats demonstrated that DMC-GF achieved an 8.5-fold increase in brain-to-blood concentration ratio two hours post-intravenous administration, markedly superior to the 0.2-fold increase observed with DMC-BH. In vitro assays showed that DMC-GF exerted a more substantial inhibitory effect on GSC proliferation than DMC-BH ($p < 0.01$), as assessed by Cell Counting Kit-3D and EdU assays. Mechanistic analysis via the Kyoto Encyclopedia of Genes and Genomes (KEGG) pathway indicated that DMC-GF's anti-GSC activity is associated with disruption of mitochondrial oxidative phosphorylation. Treatment with DMC-GF at a concentration of 4 μM caused a notable decrease in mitochondrial membrane potential and maximal mitochondrial oxygen consumption. Additionally, exposure to 8 μM DMC-GF led to a marked ($> 70\%$) reduction in SLC25A1, a mitochondrial citrate transporter, protein levels ($p < 0.01$). Overexpression of SLC25A1 attenuated both the decreased proliferation and enhanced apoptosis caused by DMC-GF ($p < 0.01$). Furthermore, the proteasome inhibitor MG132 (10 μM) and TRIM33, an E3 ubiquitin ligase involved in proteasome-mediated protein degradation, knockdown via shRNA both abrogated the DMC-GF-mediated decrease in SLC25A1 protein levels ($p < 0.05$). These findings underscore the potential of DMC-GF as an efficacious targeted therapeutic against GSCs, offering enhanced brain specificity and stability, and elucidating its mechanism involving mitochondrial dysfunction and SLC25A1 degradation.

Keywords DMC-BH, DMC-GF, Glioma stem cells, GLUT1, SLC25A1

[†]Lei Shi, Xifeng Fei, Jian Huang, Bao He and Zhixiang Sun contributed equally to this work.

*Correspondence:

Guan Sun
710020210058@xzhmu.edu.cn

¹Department of Neurosurgery, Affiliated Kunshan Hospital of Jiangsu University, China Medical University, Gusu School, Nanjing Medical University, Suzhou, P. R. China

²Department of Neurosurgery, Suzhou Kowloon Hospital, Shanghai Jiaotong University School of Medicine, Suzhou, P. R. China

³Department of Emergency Medicine, Affiliated Kunshan Hospital of Jiangsu University, China Medical University, Gusu School, Nanjing Medical University, Suzhou, P. R. China

⁴Department of Neurosurgery, The Yancheng Clinical College of Xuzhou Medical University, The First people's Hospital of Yancheng, Yancheng, P. R. China



© The Author(s) 2025. **Open Access** This article is licensed under a Creative Commons Attribution-NonCommercial-NoDerivatives 4.0 International License, which permits any non-commercial use, sharing, distribution and reproduction in any medium or format, as long as you give appropriate credit to the original author(s) and the source, provide a link to the Creative Commons licence, and indicate if you modified the licensed material. You do not have permission under this licence to share adapted material derived from this article or parts of it. The images or other third party material in this article are included in the article's Creative Commons licence, unless indicated otherwise in a credit line to the material. If material is not included in the article's Creative Commons licence and your intended use is not permitted by statutory regulation or exceeds the permitted use, you will need to obtain permission directly from the copyright holder. To view a copy of this licence, visit <http://creativecommons.org/licenses/by-nc-nd/4.0/>.

Introduction

Glioblastoma multiforme (GBM) constitutes the most lethal form of adult brain cancer, with a dismal 5-year survival rate of less than 6.9% [1]. Currently, the clinical strategy involves a combination of surgical resection followed by radiotherapy and temozolomide chemotherapy. This approach extends the median survival time of patients from 2 to 3 months to only 12–14 months [2]. Several obstacles impede the effective management of GBM. For example, surgical resection would be insufficient when cancer cells invade and disperse beyond the tumour mass identifiable via clinical imaging. Additionally, many potentially therapeutic agents are hindered by their inability to permeate the blood-brain barrier, and the inherent radioresistance of the tumour tissue further compounds the challenge.

Furthermore, although glioma cells are highly aggressive, a subpopulation of cells—referred to as glioma stem cells (GSCs)—plays an especially pivotal role in treatment resistance and tumour relapse. GSCs possess stem-like properties, including self-renewal and multipotency, which enable them to replenish the bulk tumour mass and survive conventional therapies. These cells are often more resilient to chemotherapy and radiotherapy due to enhanced DNA repair mechanisms and resistance to apoptosis. Consequently, targeting GSCs is a critical strategy to improve patient outcomes by potentially preventing tumour regrowth and overcoming therapeutic resistance.

Mounting evidence points towards the existence of glioma-initiating cells (GICs), also known as glioma stem cells (GSCs), within GBM [3]. These GSCs exhibit a profound resistance to both chemotherapy and radiotherapy, which exacerbates the drug resistance and recurrence associated with GBM [4]. Current clinical trials often fail to address the underlying GSC population, highlighting a pressing need to develop agents designed to eradicate these highly tumorigenic cells. Developing efficacious therapeutics aimed at GSCs could potentially overcome the drug resistance and recurrence plaguing GBM management [5]. However, investigations into drug discovery targeting GSCs and elucidating their biological mechanisms are scant within the academic landscape. There is an unequivocal need for further research and exploration to identify novel therapeutic targets and devise effective treatment strategies.

In prior research, we established that the curcumin pyrrolidine derivative, DMC-BH, displays noteworthy anti-GSC activity both *in vivo* and *in vitro* [6]. Nevertheless, DMC-BH faces several substantial hurdles that inhibit its further progression to preclinical development: (1) Limited potency against tumour cells: Its efficacy against GSCs is currently not optimal, potentially resulting in tumour recurrence and drug resistance in

subsequent stages. (2) Suboptimal metabolic stability: DMC-BH exhibits rapid clearance *in vivo*, with a plasma half-life of a mere 1.5 hs following intraperitoneal injection. This quick metabolism leads to a short therapeutic window. (3) Inadequate brain-targeting: While DMC-BH can partially cross the blood-brain barrier, the achieved concentration within the brain is not therapeutically effective. The drug's systemic distribution not only mitigates its potential curative impact but also poses a risk of systemic toxicity. Given these challenges, there is a pressing need to devise innovative approaches and strategies to enhance DMC-BH's brain targeting and metabolic stability. Improvements in these areas could augment its therapeutic efficacy, facilitating precise treatment strategies for glioma.

The blood-brain barrier (BBB) constitutes a tightly woven network of brain capillary endothelial cells, basement membrane, neighbouring pericytes, astrocytes, and microglia [7]. It imposes unique druggability constraints for therapeutic drugs targeting gliomas, distinguishing them from non-brain tumours. Diverse endogenous carrier transporter proteins on the capillary endothelial cells of the BBB, such as glucose, amino acid, and peptide transporters, facilitate the transport of nutrients like glucose, amino acids, and nucleotides into the brain [8]. These nutrients cannot freely diffuse into the brain, making these transporters instrumental in increasing their effective concentration [9]. The design and modification of drug molecules to utilize these transport mechanisms has emerged as a crucial strategy for improving pharmacokinetics, enhancing CNS penetration, and ultimately providing more effective treatment options.

From a clinical standpoint, there remains a dire unmet need for new therapeutics to cross the BBB, target GSCs, and minimize systemic toxicity. Given the significant clinical burden of recurrent GBM and the shortcomings of current therapies in eradicating GSCs, novel agents capable of brain targeting hold high potential for improving patient survival and quality of life.

Glucose transporter type 1 (GLUT1) is the most crucial and abundant on the BBB, surpassing other transporters by a factor of 15–3000 [10]. GLUT1's primary function is to deliver glucose to the brain, maintaining brain energy metabolism [11]. Studies indicate that brain tumorigenesis prompts heightened GLUT1 expression on the BBB due to accelerated metabolism and nutrient requirements, strengthening the premise for designing GLUT1-based brain-targeted anti-glioma drugs. Interestingly, glucose, as GLUT1's exclusive substrate, does not form a pivotal hydrogen bond at the binding site for affinity during transportation, suggesting that the 6-hydroxyl group could be a potential attachment site for designing brain-targeting molecules (see Fig. 1A) [12].

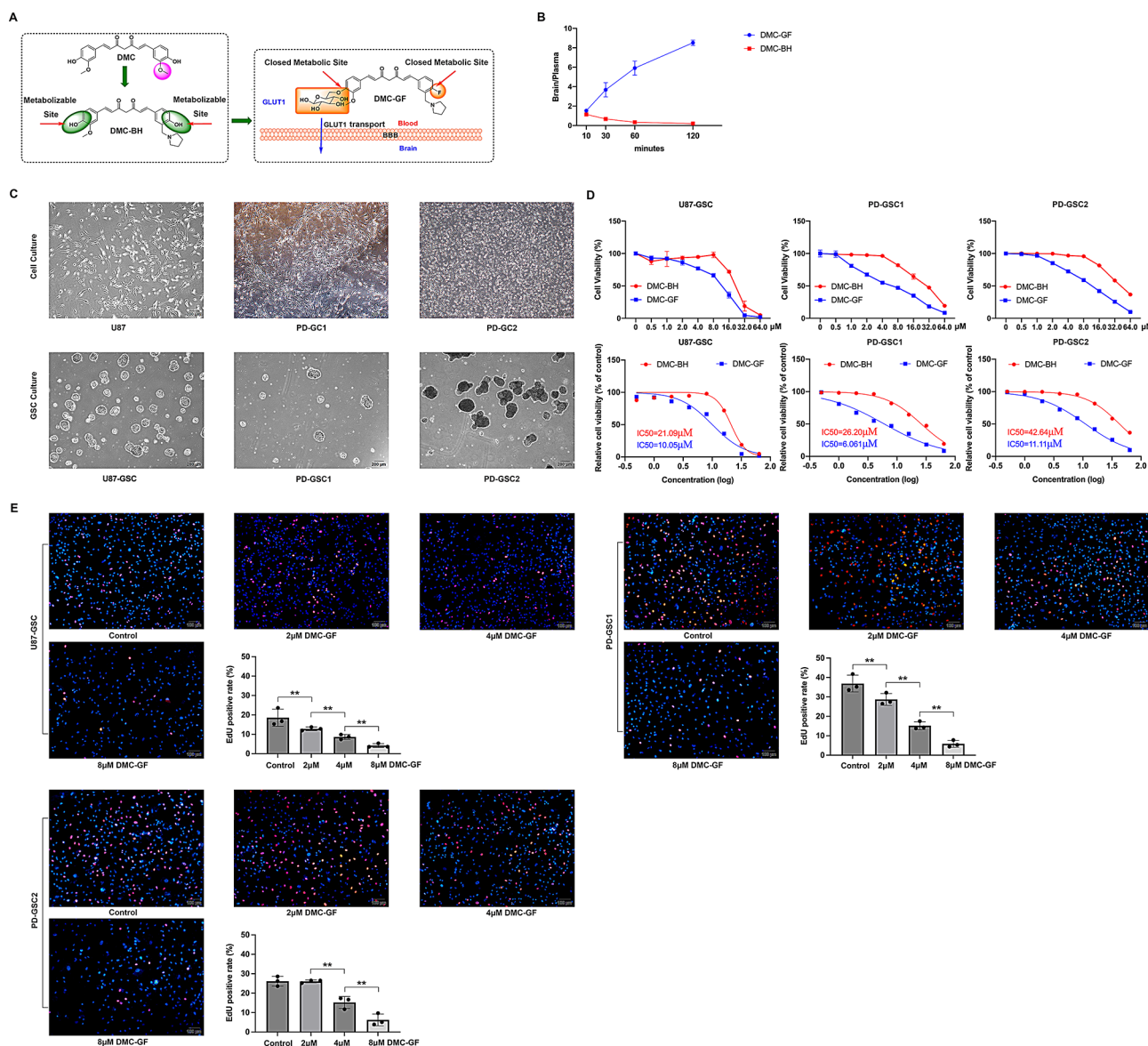


Fig. 1 Verification of DMC-GF Structure and its Pharmacological Impact. **(A)** Structural depiction of the engineered DMC-GF molecule. **(B)** Assessment of blood-brain barrier (BBB) permeability in rats. **(C)** Cultivation of U87-GSC alongside PD-GSC1 and PD-GSC2 for subsequent pharmacological assessments. **(D)** Cell viability and IC₅₀ of U87-GSCs, JZL2301103-GSCs and JZL2301206-GSCs after exposure to different concentrations of DMC-BH and DMC-GF for 24 h were analyzed by CCK-8 assays ($n = 5$). **(E)** The EdU positive rate in U87-GSC, PD-GSC1 and PD-GSC2 after treatment with different concentrations of DMC-BH and DMC-GF for 24 h ($n = 3$). Three independent biological replicates were included for (E). **, $P < 0.01$

Earlier, we conducted an exhaustive pharmacokinetic study on DMC-BH molecules [13]. The findings revealed that two exposed phenolic hydroxyl groups in DMC-BH renders it susceptible to Phase II metabolism, resulting in low in vivo exposure. Pursuing a “closed metabolic site” drug design strategy, we replaced the phenolic hydroxyl group adjacent to the pyrrolidinyl group with a fluorine atom, blocking the metabolic site and curbing metabolism. Concurrently, we substituted the phenolic hydroxyl group adjacent to the methoxy group with glucose, achieving a dual objective: blocking the metabolic site and transforming DMC-BH into a GLUT1 substrate. This

transformation allows GLUT1 on the BBB to recognize and transport it into the brain, thereby augmenting the effective concentration in the brain. Based on the above research, we designed a novel brain-targeting molecule, DMC-GF, by linking the metabolizable phenolic hydroxyl group in DMC-BH to the 6-position of glucose (as illustrated in Fig. 1A). We expect that this alteration will facilitate DMC-GF’s recognition by GLUT1, its translocation into the brain, and its robust anti-glioma activity.

Therefore, the present study was undertaken to evaluate the therapeutic potential of DMC-GF against GSCs; this study aimed to elucidate the impact of DMC-GF on

GSCs, complemented by validation experiments in intracranial orthotopic tumour xenograft models. By targeting glioma stem cells and achieving efficient brain penetration, we aim to provide a clinically meaningful therapeutic strategy for GBM patients facing dismal prognoses. Additionally, we delved into DMC-GF's potential mechanistic role within GSCs. The findings from these investigations could shed light on the influence of DMC-GF on GSCs, carving a new research trajectory in the therapeutic application of DMC-GF against GSCs.

Materials and methods

Primary glioma cell culture

In this experiment, primary glioma cells were isolated and cultured from surgically resected specimens of glioblastoma patients. Briefly, glioma tissue samples are collected from patients undergoing surgery or biopsy after obtaining informed consent. The collected tissue is minced into 1–2 mm small pieces and enzymatically digested using trypsin (#BL501A, Biosharp, China) to dissociate the cells from the extracellular matrix. Viable glioma cells are then seeded into culture vessels coated with Matrigel Basement Membrane Matrix (#356234, Corning, USA) and cultured in a DMEM/F12 medium (#11320033, Gibco, USA) supplemented with 15% fetal bovine serum (#10091148, Gibco, USA) and 1% penicillin-streptomycin (PS) (100 U/ml penicillin and 100 mg/ml streptomycin) (#BL505A, Biosharp, China) at 37 °C with a humidified atmosphere of 5% carbon dioxide (CO₂). This study has obtained approval and consent from the Institutional Review Board (IRB) of the Affiliated Kunshan Hospital of Jiangsu University (2021-06-004-H01).

Glioma stem cell culture

U87 cells were purchased from the Cell Bank of Shanghai Academy of Sciences. To culture GSCs, GSCs were isolated and cultured using neurosphere formation assays (#P2401, QiDa Biotechnology, Shanghai, China). Following the manufacturer's instructions, GSCs were suspended in a serum-free medium supplemented with growth factors (#HUXNF-90011, Cyagen Biosciences, China). The medium was refreshed every 2–3 days, and neurospheres could be passaged through mechanical dissociation [14]. The stemness of the cells was assessed by characterizing the expression of stem cell markers, including CD133 (#CL488-18470, Wuhan Sanying, China) and Nestin (#CL594-19483, Wuhan Sanying, China) [15, 16].

Cell counting kit-3D assay

To assess the inhibitory effect of DMC-GF on stem cell sphere proliferation, the Cell Counting Kit-3D kit (#C0049L, Beyotime Biotechnology, Shanghai, China) was utilized. Glioma stem cells (GSCs) were seeded at

a density of 200 cells per well in 200 µL of non-serum medium within a 96-well plate. Subsequently, 10 µL of the CCK-3D reagent was added, followed by incubation in a cell culture incubator for 0.5–3 h. The gentle tapping of the plate ensured proper mixing of the orange-yellow formazan within each well, and the absorbance at 450 nm was measured.

EdU assay

Single cells dissociated from glioblastoma stem-like cell tumour spheres were plated on 96-well plates and exposed to 100 µL of medium containing 50 µM EdU (#C10310-1, RIBO BIO, Guangzhou, China). Following incubation at 37 °C with 5% CO₂ for 2 h, the cells were fixed with 4% paraformaldehyde (#P0099, Beyotime Biotechnology, China) for 30 min and subsequently treated with 0.5% Triton-X-100 (#BL2203A, Biosharp, China) in PBS (#BL2215A, Biosharp, China) for 20 min. Following the incubation period, 100 µL of Apollo staining reaction solution (#C10310-1, RIBO BIO, Guangzhou, China) was added to each well, and nuclei were stained with Hoechst dye (#C10310-1, RIBO BIO, Guangzhou, China). The proliferation rate was assessed according to the manufacturer's instructions, utilizing the Cell-Light EdU Apollo567 In Vitro Kit (#C10310-1, RIBO BIO, Guangzhou, China). Fluorescence images capturing the incorporation of EdU were obtained using a Leica fluorescence microscope. This experiment was repeated three times to ensure reproducibility.

Annexin V-APC cell apoptosis detection assay

To perform the Annexin V-APC Cell Apoptosis Detection assay (#KGA1107-100, KeyGEN Biotech., Nanjing, China), cells were cultured in appropriate growth media at 37 °C with 5% CO₂ until they reached 70–80% confluency. After treatment with apoptotic inducers, cells were harvested using trypsin-EDTA and pelleted by centrifugation at 300–400×g for 5 min at 4 °C. The harvested cells were washed with cold PBS and resuspended in binding buffer at a concentration of $1-5 \times 10^6$ cells/mL. A 100 µL of the cell suspension ($1-5 \times 10^5$ cells) was transferred to a new tube, and 5 µL of Annexin V-APC solution was added. The cells were gently mixed and incubated at room temperature for 10–15 min, protected from light. For PI staining, 5 µL of PI solution was added and incubated for 5 min. Following staining, 400 µL of binding buffer was added for dilution, and flow cytometry analysis was performed using appropriate detectors for Annexin V-APC and PI. Flow cytometry analysis software determined the percentage of cells in different apoptosis stages.

TUNEL cell apoptosis detection assay

To perform the TUNEL Cell Apoptosis Detection assay (#BL644B, Biosharp, Anhui, China), cells were cultured in suitable growth media at 37 °C with 5% CO₂ until they reached the desired confluency (i.e., approximately 70–80% confluency, meaning that the majority of the culture surface is covered by cells without overgrowth). After treatment with apoptotic inducers, cells were fixed with 4% paraformaldehyde for 15–30 min at room temperature. Following fixation, cells were washed with PBS and permeabilized with 0.1% Triton X-100 in PBS for 5–15 min. After washing, the cells were incubated with the TUNEL reaction mixture containing terminal deoxynucleotidyl transferase (TdT) enzyme and fluorescein-labeled nucleotides for 1–2 hs at 37 °C in a humidified chamber. The reaction was stopped by washing the cells with PBS. For nuclear counterstaining, cells were incubated with Hoechst dye for 10 min. Finally, the cells were mounted on slides and visualized using fluorescence microscopy.

Measurement of oxidative phosphorylation and Glycolysis

Real-time measurements of cellular oxygen consumption rate (OCR) and extracellular acidification rate (ECAR) were performed using the Seahorse XF96 Extracellular Flux Analyzer (Seahorse Bioscience, North Billerica, MA, USA). In brief, cells were exposed to 4 μM DMC-GF for 12 hs before being plated into Seahorse custom cell plates. Following probe calibration, OCR was assessed through the sequential injection of the following mitochondrial respiration regulators: oligomycin (ATP synthase inhibitor; 1 μM), FCCP (uncoupler; 1 μM), rotenone (complex I inhibitor; 1 μM), and antimycin A (complex III inhibitor; 1 μM). The cellular glycolysis profile under aerobic conditions was determined by measuring ECAR in cells treated with DMC-GF. Measurements were taken after the sequential injection of glucose (10 mM), oligomycin (1 μM), and 2-DG (100 mM).

Quantitative real-time PCR (qRT-PCR)

SYBR Green PCR Master Mix (Takara) was used for quantitative real-time PCR (qRT-PCR). The forward primer sequence for SLC25A1 is 5'-CCCCATGGAGACC ATCAAG-3', and the reverse primer sequence is 5'-CCT GGTACGTCCTTCAG-3'. For the housekeeping gene ACTB, the forward primer sequence is 5'-GGCTGTATT CCCCTCCATCG-3', and the reverse primer sequence is 5'-CCAGTTGGTAACAATGCCATGT-3'. The qRT-PCR was performed using a StepOnePlus Real-Time PCR System (Applied Biosystems). The reaction conditions were set as follows: initial denaturation at 95 °C for 10 min, followed by 40 cycles of denaturation at 95 °C for 15 s and annealing/extension at 60 °C for 1 min. Gene expression levels were normalized to ACTB and calculated using the

2^{-ΔΔCt} method. All experiments were conducted in triplicate to ensure reproducibility.

Western blot assay

To perform the Western blot assay, protein samples were prepared by lysing the cells or tissues in a RIPA lysis buffer containing protease inhibitors (#P0038, Beyotime Biotechnology, Shanghai, China). The lysates were then centrifuged at 12,000 × g for 10–15 min at 4 °C to remove cellular debris. Proteins were separated by running the gel at 100 V until the desired separation was achieved. Following electrophoresis, proteins were transferred onto the PVDF membrane using a wet transfer apparatus at 300 mA for 60 min. The membrane was then blocked with 5% non-fat milk in Tris-buffered saline with Tween-20 (TBST) for 1 h at room temperature to prevent non-specific binding. After blocking, the membrane was incubated overnight with a primary antibody specific to the target protein of interest at 4 °C. Protein bands were visualized using ECL Chemiluminescence Substrate (#BL520B, Biosharp, Anhui, China), and the signals were captured using a chemiluminescence imaging system. The band intensities were quantified using densitometry software, and the protein expression levels were normalized to a loading control such as GAPDH.

The primary antibodies included rabbit anti-Bax (#ab32503, 1:1000, abcam, UK); rabbit anti-Bad (#ab32445, 1:1000, abcam, UK); rabbit anti-caspase-3 (#ab32351, 1:1000, abcam, UK), cleaved-caspase-3 (#ab32042, 1:1000, abcam, UK), rabbit anti-Bcl-2 (#ab182858, 1:1000, abcam, UK), rabbit anti-Bcl-xL (#ab32370, 1:1000, abcam, UK), mouse anti-NDUFB8 (#67690-1-Ig, 1:1000, Wuhan Sanying, China), mouse anti-SDHB (#67600-1-Ig, 1:1000, Wuhan Sanying, China), mouse anti-UQCRC2 (#67547-1-Ig, 1:1000, Wuhan Sanying, China), mouse anti-COX II (#68527-1-Ig, 1:1000, Wuhan Sanying, China) and rabbit anti-ATP5A (#14676-1-AP, 1:1000, Wuhan Sanying, China), rabbit anti-SLC25A1 (#15235-1-AP, 1:1000, Wuhan Sanying, China), rabbit anti-TRIM33 (#55374-1-AP, 1:1000, Wuhan Sanying, China), and rabbit anti-GAPDH (#10494-1-AP, 1:1000, Wuhan Sanying, China). The secondary antibody was horseradish peroxidase (HRP)-conjugated anti-rabbit (1:5000, ZSGBBIO, China) and anti-mouse (1:5000, Thermo Fisher Scientific, USA).

SLC25A1, TRIM33 knockdown and overexpression lentiviral vectors

To investigate the functional role of SLC25A1, we employed both knockdown and overexpression strategies in GSCs. For knockdown, lentiviral vectors encoding short hairpin RNA (shRNA) specific for SLC25A1 (sh-SLC25A1, CAT. No. Q9994-1, targeting sequence: 5'-CCATCCGCTTCTTCGTCATGA-3') and a non-target

shRNA control (sh-NC-SLC25A1) were purchased from GenePharma (Shanghai, China). Additionally, to explore the role of TRIM33, we utilized a lentiviral vector encoding shRNA specific for TRIM33 (sh-TRIM33, CAT. No. Q9994-2, targeting sequence: 5'-GCGACTGATTACTT TCCAGTT-3') and a corresponding non-target shRNA control (sh-NC-TRIM33), also obtained from GenePharma (Shanghai, China). For overexpression, we utilized a lentiviral vector carrying the open reading frame (ORF) of the human SLC25A1 sequence (OE-SLC25A1, CAT. No. Q9980) and a corresponding empty vector control (OE-NC). The viral particles were produced by co-transfecting HEK293T cells with shuttle plasmids and packaging plasmids (pGag/Pol, pRev, pVSV-G) according to the manufacturer's instructions. After 48 h, the supernatant containing lentiviral particles was collected, filtered, and used to infect the GSCs in the presence of 8 µg/mL Polybrene (Sigma-Aldrich, USA).

Human orthotopic patient-derived xenograft (PDX) model

All animal experiments were performed in accordance with the ARRIVE guidelines and approved by the Institutional Animal Care and Use Committee (IACUC). There were 6 nude mice in each group, and the maximum and minimum values were removed during statistics. Surgically resected glioma tissues were immediately cut into small fragments (approximately 2–3 mm³) and enzymatically dissociated to obtain patient-derived glioma stem cells (GSCs).

For intracranial tumour establishment, 5×10^5 patient-derived GSCs were suspended in 5 µL of PBS and stereotactically injected into the right striatum of SCID mice (4–6 weeks old, ~20 g). The coordinates used were 2.0 mm lateral to the bregma and 3.0 mm depth, guided by a stereotactic frame. About 7 days post-injection, mice were randomly assigned (via a random number generator) to receive DMC-GF (20 mg/kg, i.p.) once daily or vehicle control for 14 consecutive days, with blinding maintained through coded treatment vials.

On day 14 post-injection, mice underwent T2-weighted cranial MRI scanning to evaluate tumour size and location. Immediately following the MRI, mice were euthanized by CO₂ inhalation, and whole brains were harvested for histological, molecular, or immunohistochemical analyses. All mice were maintained under specific pathogen-free (SPF) conditions (22–24 °C, 40–60% humidity, 12-h light/dark cycle) with ad libitum access to standard chow and water. Any animals exhibiting severe neurological deficits, excessive weight loss (>20%), or signs of distress were euthanized before the 14-day endpoint to minimize suffering, in compliance with our IACUC-approved protocol.

Statistical analyses

Statistical analyses were performed using GraphPad Prism 5.0 software (San Diego, CA, USA). For experiments involving more than two groups, we performed one-way or two-way ANOVA followed by Tukey's post-hoc test to correct for multiple comparisons. When data were collected over multiple time points from the same subjects, we used repeated-measures ANOVA with an appropriate post-hoc adjustment for multiple comparisons. For comparisons between two groups with equal variances, an unpaired t-test was used. If the variances were not equal, the Mann-Whitney U test was employed. * $p < 0.05$ and ** $p < 0.01$ were considered statistically significant in all analyses. Quantitative data are presented as the mean ± standard deviation (SD), unless stated otherwise.

Results

Structural verification and preliminary Pharmacological studies of DMC-GF

Adopting the pharmaceutical design principle of encapsulating metabolic sites [17], we engineered DMC-GF and verified its molecular structure as depicted in Fig. 1A. Subsequent in vivo assessments of blood-brain barrier (BBB) permeability in rats demonstrated a notable enhancement in the brain-to-blood concentration ratio of DMC-GF, achieving an 8.5 fold increase two hs following intravenous administration. This represents a significant advancement over its progenitor molecule, DMC-BH, which manifested a mere 0.2 fold increase under identical conditions, underscoring DMC-GF's superior capacity for brain entry, potentially facilitated by the GLUT1 transporter, as evidenced in Fig. 1B. Further investigations involved the cultivation of U87 stem cells (U87 GSC) alongside two primary glioma cell lines, PD-GC1 and PD-GC2, as illustrated in Fig. 1C. Comparative analyses of DMC-GF's anti-glioblastoma stem cell (GSC) efficacy, utilizing CCK-8 assays as shown in Fig. 1D, revealed a marked inhibition of tumour cell proliferation relative to DMC-BH. Additional EdU incorporation assays indicated a significant reduction in the EdU positive rate within the DMC-GF treatment cohort, suggesting a robust inhibitory effect on GSC proliferation, detailed in Fig. 1E. Taken together, these outcomes firmly position DMC-GF as an improvement over its precursor, DMC-BH, in terms of biological activity and brain permeability, thereby laying a foundational basis for ensuing investigative endeavours.

DMC-GF-induced cell apoptosis in GSCs

To investigate the pro-apoptotic efficacy of DMC-GF on glioblastoma stem cells (GSCs), we embarked on a series of in vitro experiments. Initially, a spectrum of GSC lines was subjected to various concentrations of DMC-GF,

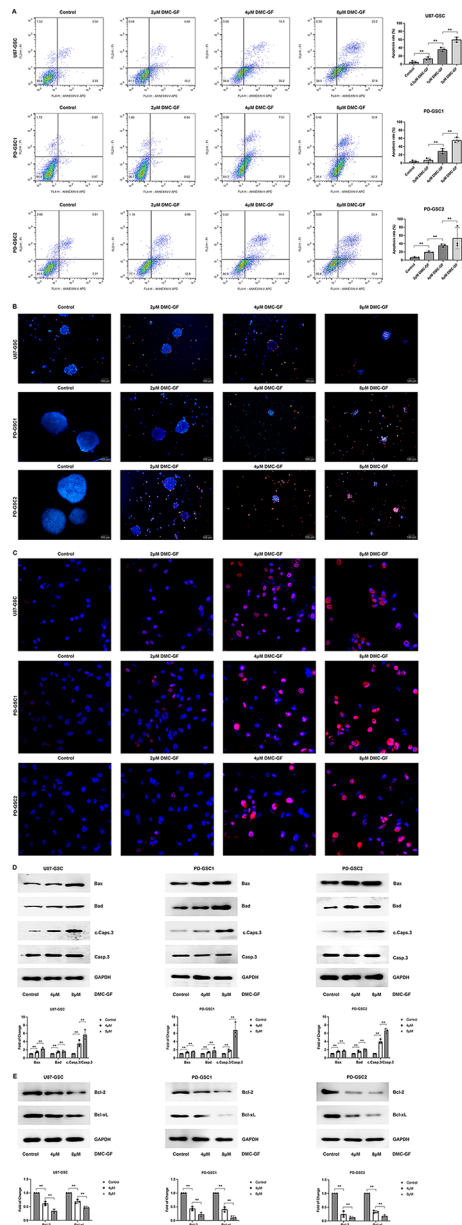


Fig. 2 DMC-GF induced cell apoptosis in glioblastoma stem cells (GSCs). **(A)** The apoptosis rate of U87-GSC, PD-GSC1 and PD-GSC2 treated with DMC-GF for 24 h was detected by flow cytometry assays ($n=3$). **(B)** The decrease in spheroid size and the dose-dependent increase in TUNEL-positive cells in GSC-spheroids after treatment with different concentrations of DMC-GF for 24 h ($n=3$). **(C)** Single-cell suspensions of GSC spheroids treated with DMC-GF, prepared and distributed into a 96-well plate for observation and validation ($n=3$). **(D)** Expression levels of pro-apoptotic proteins (Bax, Bad, cleaved Caspase-3) in GSCs after exposure to DMC-GF for 48 h were analyzed by Western blot ($n=3$). **(E)** Expression levels of anti-apoptotic proteins (Bcl-2, Bcl-xL) in GSCs after exposure to DMC-GF for 48 h were analyzed by Western blot ($n=3$). Three independent biological replicates were included. **, $P<0.01$

followed by flow cytometric analysis employing Annexin V/Propidium Iodide staining to delineate the population of cells in the early and late stages of apoptosis. Results depicted in Fig. 2A elucidate that DMC-GF administration notably propels apoptosis in GSCs, with a dose-dependent augmentation in apoptotic rates correlating with increasing concentrations of DMC-GF. To corroborate the induction of apoptosis by DMC-GF, a Terminal deoxynucleotidyl transferase dUTP nick end labeling (TUNEL) assay was conducted, aiming to detect and quantify apoptotic DNA fragmentation. As illustrated in Fig. 2B, the assay's outcomes reveal a diminution in stem cell spheroid dimensions alongside a dose-dependent increase in the proportion of TUNEL-positive cells, signifying apoptosis. To enhance observational clarity and validation, GSC spheroids were dissociated into single-cell suspensions and allocated into a 96-well plate, as demonstrated in Fig. 2C.

Beyond the assessment of cell mortality, our investigation extended to the mechanistic bases underlying apoptosis induced by DMC-GF. We scrutinized the expression of pivotal proteins within apoptotic pathways, employing western blot analysis to quantify the levels of pro-apoptotic proteins (including Bax, Bad, and Caspase-3) and anti-apoptotic proteins (such as Bcl-2 and Bcl-xL) in GSCs post-DMC-GF application. Illustrated in Fig. 2D, our findings disclose a pronounced elevation in the pro-apoptotic proteins Bax, Bad, and cleaved Caspase-3 subsequent to DMC-GF treatment. Concurrently, a discernible reduction in the anti-apoptotic proteins Bcl-2 and Bcl-xL was observed, as evidenced in Fig. 2E. These comprehensive in vitro analyses suggest that DMC-GF could effectively induce apoptosis in GSCs, potentially mediated by the modulation of key apoptotic proteins. Further studies will be beneficial to elucidate the molecular intricacies of DMC-GF's action fully.

Effects of DMC-GF on GSCs mitochondrial respiration function

To further study the mechanism and potential targets of DMC-GF, we conducted mRNA-seq research on GSCs treated with DMC-GF and performed pathway analysis on related differential genes ($FC \geq 2$, $P \leq 0.05$) by Kyoto Encyclopedia of Genes and Genome (KEGG), and found that the differential genes mainly Enriched in Glycosaminoglycan degradation, Glycolysis / Gluconeogenesis and Oxidative phosphorylation related pathways (Fig. 3A, B). Oxidative phosphorylation is a biochemical process that occurs in eukaryotic cells' inner mitochondrial membrane or in prokaryotic organisms' cytoplasm [18]. It is a coupling reaction in which the energy released when substances are oxidized in vivo supplies ADP and inorganic phosphoric acid to synthesize ATP through the respiratory chain. It is speculated that the role of DMC-GF may

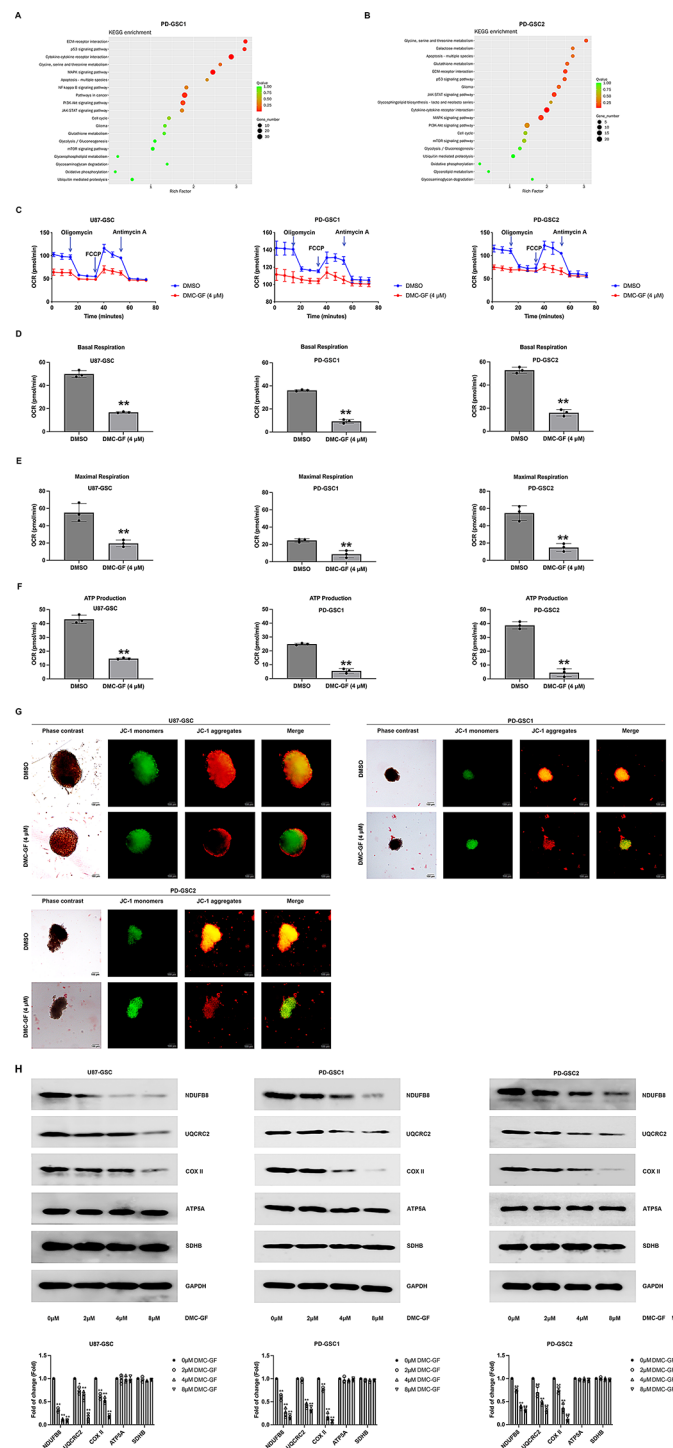


Fig. 3 DMC-GF inhibits GSCs' mitochondrial respiration function. **(A, B)** Differential gene expression analysis of PD-GSC1 and PD-GSC2 was treated with DMC-GF using mRNA-seq, and pathways analysis was conducted by KEGG. **(C)** Evaluation setup for mitochondrial functions including basal respiration, maximal respiration, and ATP production in GSCs post-DMC-GF treatment ($n=6$). **(D)** Basal respiration rates in GSCs after treatment with DMC-GF ($n=3$). **(E)** Maximal respiration rates in GSCs upon FCCP addition ($n=3$). **(F)** ATP production in GSCs after treatment with DMC-GF ($n=3$). **(G)** Mitochondrial membrane potential analysis after treatment with DMC-GF measured by JC-1 staining method ($n=3$). **(H)** Western blot analysis of the abundance of mitochondrial electron transport chain (ETC) complexes NDUFB8, SDHB, UQCRC2, COX II, and ATP5A in GSCs post-DMC-GF treatment compared with 0 μ M DMC-GF treatment group ($n=3$). Three independent biological replicates were included for **(D)–(H)**. **, $P<0.01$

be related to mitochondrial function and cellular energy metabolism. We then evaluated mitochondrial functions, including basal respiration, maximal respiration, and ATP production after DMC-GF treatment (Fig. 3C). As shown in Fig. 3D, DMC-GF markedly decreased basal respiration, indicating reduced mitochondrial OXPHOS activity. Upon FCCP addition, a surge in cellular oxygen consumption was observed, which was suppressed by ETC inhibitors rotenone and antimycin A, targeting complex I and III, respectively. Concurrently, DMC-GF significantly diminished maximal respiration (Fig. 3E). Moreover, ATP production was further calculated and showed DMC-GF (4 μ M) significantly reduced ATP production (Fig. 3F). Analysis of mitochondrial membrane potential showed that compared with the control group and the DMC-GF-treated group, the DMC-GF group had lower levels of red fluorescence, indicating decreased mitochondrial membrane potential (Fig. 3G). These findings demonstrate that DMC-GF inhibits mitochondrial respiration, leading to decreased ATP production, which consequently impedes cancer cell proliferation.

We subsequently examined the abundance of the five complexes within the mitochondrial electron transport chain (ETC), including NDUFB8, SDHB, UQCRC2, COX II and ATP5A [19]. NDUFB8 is a subunit of Complex I. It catalyzes the transfer of electrons from NADH to ubiquinone. SDHB is a subunit of Complex II or succinate dehydrogenase. It participates in the oxidation of succinate to fumarate, transferring electrons to ubiquinone. UQCRC2 subunit is part of Complex III. It facilitates the transfer of electrons from ubiquinone to cytochrome C. COX II is a subunit of Complex IV. It is responsible for the final step in the electron transport chain, transferring electrons from cytochrome C to molecular oxygen, reducing it to water. ATP5A is part of Complex V. It is responsible for synthesising ATP from ADP and inorganic phosphate using the energy generated during the electron transport chain. These complexes play a crucial role in cellular respiration, where electrons are transferred through a series of protein complexes, ultimately generating ATP. As shown in Fig. 3H, a conspicuous reduction was noted in the levels of NDUFB8, UQCRC2, and COX II in GSC cultures following DMC-GF treatment. In contrast, no discernible impact was observed on the expression of ATP5A and SDHB.

Differential analysis of SLC25A1 expression levels between glioma tissue and normal tissue

The Mitochondrial Citrate Carrier, SLC25A1, is a protein-coding gene responsible for encoding a mitochondrial citrate transporter, also known as the tricarboxylate carrier (TCC) [20]. This carrier plays a crucial role in cellular energy metabolism by facilitating the transport of citrate across the inner mitochondrial membrane. We

analyzed the expression levels of SLC25A1 in a cohort of 173 GBM tissue samples obtained from the TCGA database (<https://portal.gdc.cancer.gov/>) and 273 GBM RNA sequence data from CGGA (www.cgga.org.cn). Additionally, we used 1151 normal brain tissue samples obtained from gtexportal.org/home as controls for comparison. The limma package was used to merge, normalize, and calculate the expression difference between TCGA and CGGA GBM RNA sequence data with GTEx normal brain, respectively. The results revealed a significant upregulation of SLC25A1 expression in GBM tissues compared to normal brain tissues ($P < 0.05$) (Fig. 4A). Moreover, a comprehensive Kaplan-Meier survival analysis based on TCGA data indicated a prognostic difference between GBM patients with high SLC25A1 expression and those with low SLC25A1 expression ($P < 0.05$). However, the analysis of CGGA data did not show this difference to be significant ($P > 0.05$) (Fig. 4B).

To deepen our understanding, we delved into the realm of clinical GBM patient samples, wherein we discovered a significant elevation in the protein level expression of SLC25A1 within the tumour tissues compared to the peritumoural tissues (Fig. 4C) and normal brain tissues (Fig. 4D). In a reinforcing fashion, immunohistochemical staining analysis provided additional confirmation, visually affirming the heightened presence of SLC25A1 in GBM tumour tissue compared to normal tissue (Fig. 4E). Collectively, these comprehensive investigations have shed light upon the close association between SLC25A1 and the onset, progression, and prognosis of GBM.

Effects of DMC-GF on SLC25A1 expression in primary cultured GSCs and its xenografts

To delve deeper into the potential impact of DMC-GF on the expression level of SLC25A1, we conducted a meticulous examination of GSCs following DMC-GF treatment. Intriguingly, our in vitro experimental findings showed that the expression of SLC25A1 was significantly reduced in primary cultured GSCs after exposure to DMC-GF, which was confirmed by Western blot (Fig. 5A). This intriguing observation was further confirmed by Western blot analysis of in vivo orthotopic PDX experiments, from which xenograft tumour samples also showed reduced expression of SLC25A1 in the DMC-GF intervention group (Fig. 5B). Immunohistochemistry analyses consistently supported these results, providing additional evidence of reduced SLC25A1 expression (Fig. 5C).

Subsequent investigations aimed to elucidate the underlying mechanisms driving this effect. Surprisingly, our studies unveiled that the impact of DMC-GF on SLC25A1 expression was independent of any discernible alterations in the mRNA expression levels (Fig. 5D). This intriguing discovery points towards a potential involvement of DMC-GF in modulating the post-translational

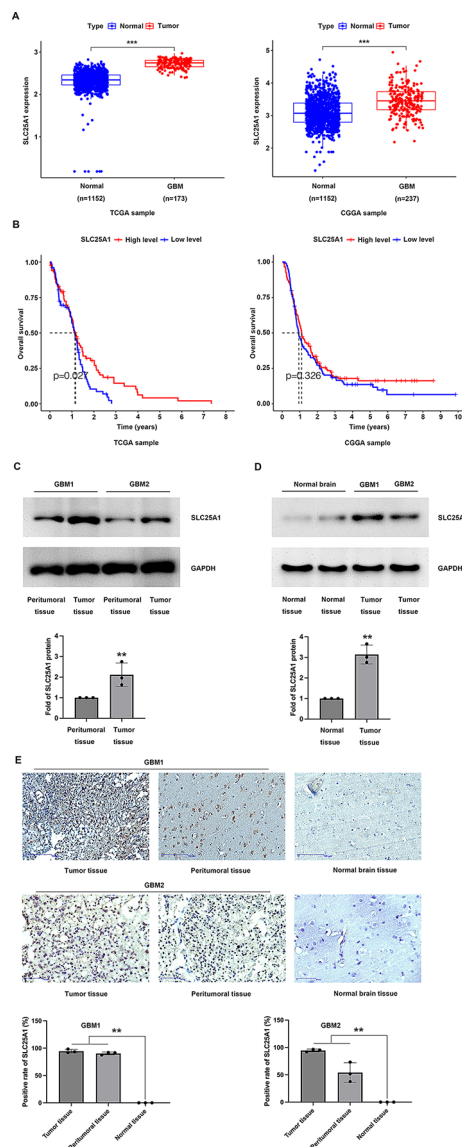


Fig. 4 Analysis of SLC25A1 expression levels in glioma tissues. **(A)** Expression levels of SLC25A1 in glioblastoma multiforme (GBM) tissue samples (173 from TCGA, 273 from CGGA) compared to normal brain tissues (1151 from GTEx) ($n=173$ GBM, $n=1151$ normal). **(B)** Kaplan-Meier survival analysis based on TCGA and CGGA data between GBM patients with high versus low SLC25A1 expression. **(C)** Protein level expression of SLC25A1 in tumour tissues compared to peritumoural tissues in clinical GBM patient samples ($n=3$). **(D)** Protein level expression of SLC25A1 in tumour tissues compared to normal brain tissues ($n=3$). **(E)** Immunohistochemical staining analysis confirming the increased presence of SLC25A1 in GBM tumour tissue compared to normal tissue. Three independent biological replicates were included for **(C)**, **(D)** and **(E)**. **, $P<0.01$

degradation process of the SLC25A1 protein. These observations collectively suggest that DMC-GF can exert a regulatory influence over the expression of SLC25A1, presenting a novel avenue for exploring the intricate interplay between DMC-GF and the protein degradation process.

SLC25A1 promotes the proliferation of GSCs

We embarked on further investigations to investigate the potential involvement of SLC25A1 in the proliferation of GSCs. Employing functional assays, we sought to elucidate the impact of SLC25A1 on GSC proliferation and its potential modulation by DMC-GF. Firstly, we employed shRNA-mediated knockdown of SLC25A1 (Genepharma, Shanghai, China) in GSCs to evaluate its effect on cell proliferation (Fig. 6A). Remarkably, the depletion of SLC25A1 resulted in a significant decrease in GSC proliferation compared to control cells (Fig. 6B). Moreover, significantly increased apoptosis rates were also observed in SLC25A1 shRNA group (Fig. 6C). And the immunohistochemical experiments conducted on the orthotopically transplanted tumours revealed a substantial reduction in the proportion of Ki67-positive cells in the SLC25A1 shRNA group (Fig. 6D). These findings suggested that SLC25A1 may play a crucial role in promoting GSC proliferation.

We conducted rescue experiments to explore the potential regulatory effect of DMC-GF on SLC25A1-mediated proliferation. GSCs were treated with DMC-GF after SLC25A1 overexpression (OE-SLC25A1) (Genepharma, Shanghai, China), aiming to restore SLC25A1 expression (Fig. 7A). Notably, the introduction of SLC25A1 overexpression partially rescued the impaired proliferation (Fig. 7B) and apoptosis (Fig. 7C) caused by DMC-GF, indicating a potential interplay between DMC-GF and SLC25A1 in GSC proliferation regulation.

To further validate the functional significance of SLC25A1 in GSCs and its potential impact on tumour growth in vivo, we conducted orthotopic Patient-Derived tumour Xenograft (PDX) experiments using PD-GSC2 with altered SLC25A1 expression. GSCs were manipulated to OE-SLC25A1 and subsequently injected into immunocompromised mice to establish orthotopic xenograft models. Remarkably, DMC-GF led to a significant reduction in tumour growth of GSCs compared to control cells (Fig. 7D). Meanwhile, we also observed a significantly increased tumour growth in DMC-GF group pretreated with OE-SLC25A1 transfection compared to the DMC-GF group. These findings suggested that SLC25A1 facilitates tumour growth within glioma stem cells (GSCs). This activity may impact how DMC-GF suppresses the development of orthotopic xenografts.

TRIM33 mediates the degradation of SLC25A1 by DMC-GF

The processes of synthesis and degradation predominantly regulate the intracellular protein level. While the mRNA level of SLC25A1 remains unaffected by DMC-GF, it suggests that DMC-GF may be involved in regulating the expression level of SLC25A1 by influencing protein degradation. To explore this further, we employed the proteasome inhibitor MG132 to intervene in GSC cells.

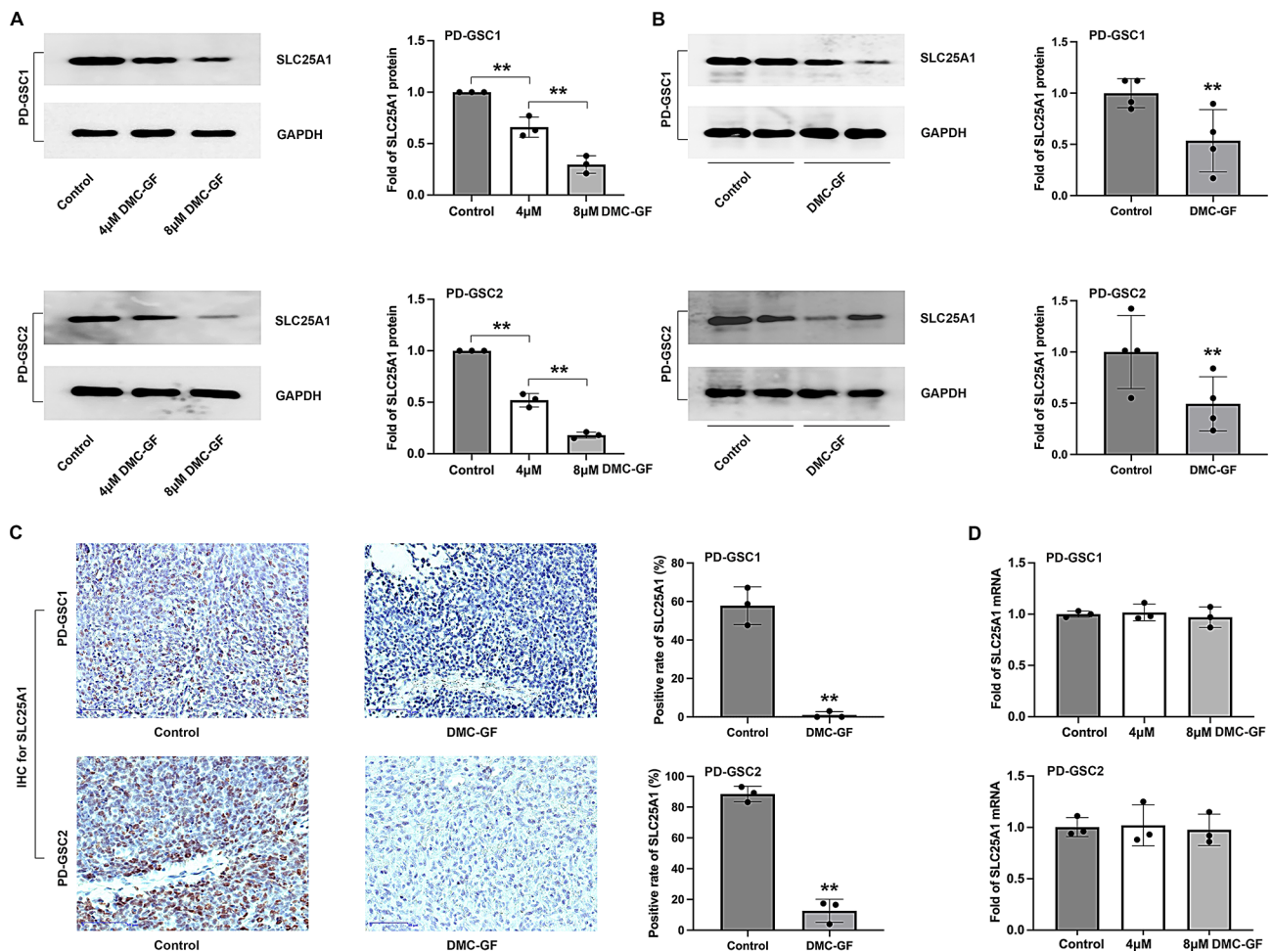


Fig. 5 DMC-GF inhibits SLC25A1 expression in primary cultured GSCs and its xenografts. **(A)** Western blot analysis of SLC25A1 expression in primary cultured GSCs after treatment with DMC-GF ($n=3$). **(B)** Western blot analysis of xenograft tumour samples indicating reduced SLC25A1 expression in the DMC-GF intervention group ($n=3$). **(C)** Immunohistochemical analysis confirming the reduced expression of SLC25A1 in xenograft tumour samples treated with DMC-GF ($n=3$). **(D)** mRNA expression levels of SLC25A1 in primary cultured GSCs post-DMC-GF treatment ($n=3$). Three independent biological replicates were included for **(A)**, **(B)** and **(C)**. **, $P<0.01$

Notably, our experimental findings revealed that the use of MG132 partially restored the protein degradation of SLC25A1 mediated by 4 μ M DMC-GF (Fig. 8A). This observation strongly suggests that DMC-GF exerts its effect on reducing the expression of SLC25A1 through a mechanism that is dependent on proteasome activity.

TRIM33, as an E3 ubiquitin ligase, marks specific proteins by ubiquitination, promoting their degradation by the proteasome. MG132, as a proteasome inhibitor, can block this degradation process, leading to the accumulation of TRIM33-marked proteins. Then, we aimed to explore whether TRIM33 is involved in the DMC-GF-mediated degradation of SLC25A1. To investigate this further, we utilized lentiviral TRIM33 shRNA (sh-TRIM33) (Genepharma, Shanghai, China) to reduce the expression of TRIM33 (Fig. 8B). Remarkably, we observed a notable reduction in the degradation effect of DMC-GF on SLC25A1 upon the suppression of TRIM33

(Fig. 8C), indicating the dependence of this process on TRIM33.

We conducted additional analysis to investigate the impact of TRIM33 on the growth of the PD-GSC2-derived PDX model. Interestingly, we observed that the inhibition of TRIM33 led to a significant enhancement in the growth of orthotopically transplanted tumours, as depicted in Fig. 8D. Furthermore, the expression of the proliferative marker Ki67 in cells was notably increased, as shown in Fig. 8E. Consistently, Western blot analysis indicated a corresponding elevation in the levels of SLC25A1, as illustrated in Fig. 8F.

Discussion

In this study, we successfully synthesized DMC-GF, a derivative of DMC-BH, employing the pharmaceutical design principle of ‘encapsulation of metabolic sites’ [17]. The structural identity of DMC-GF was verified,

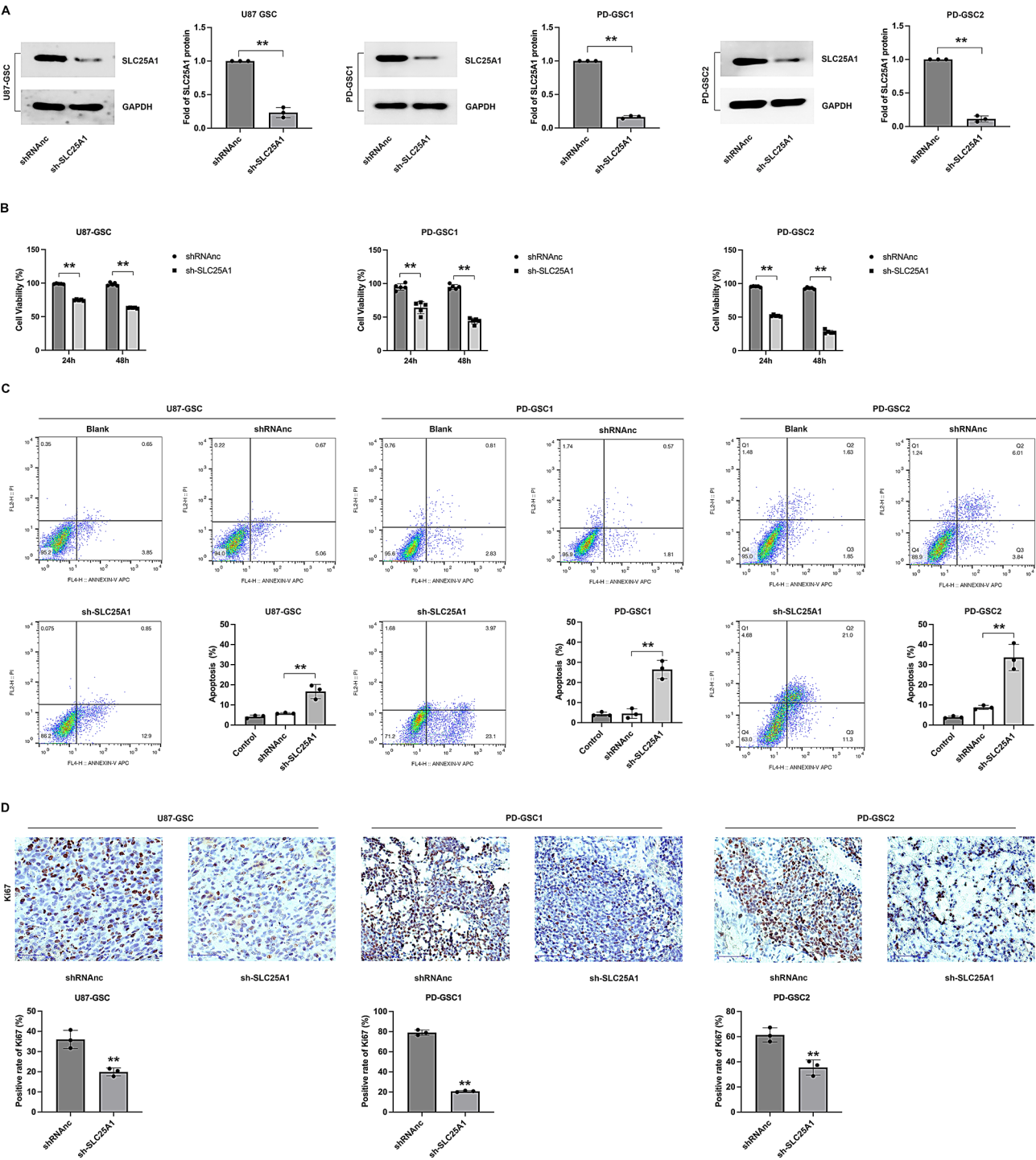
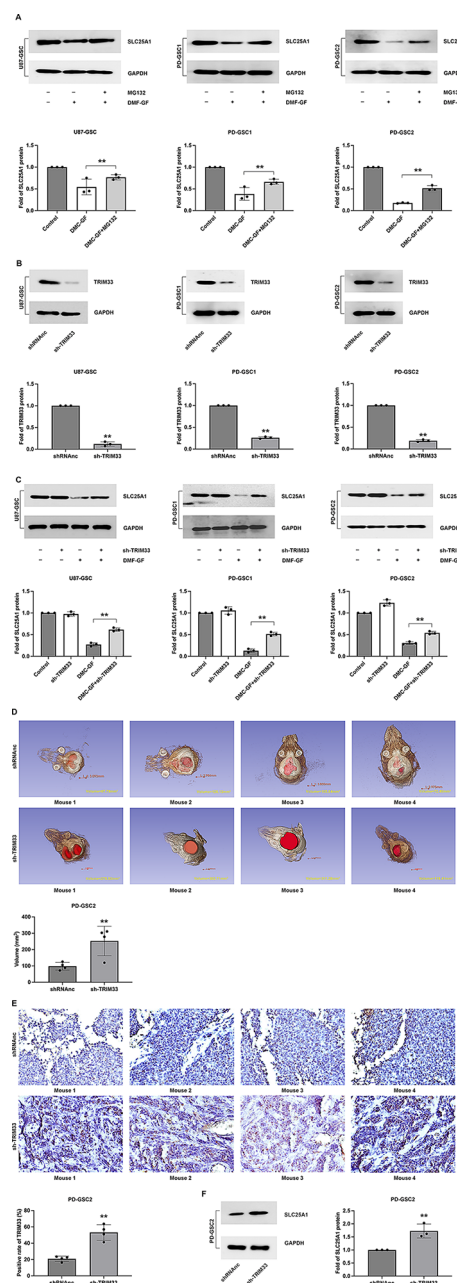
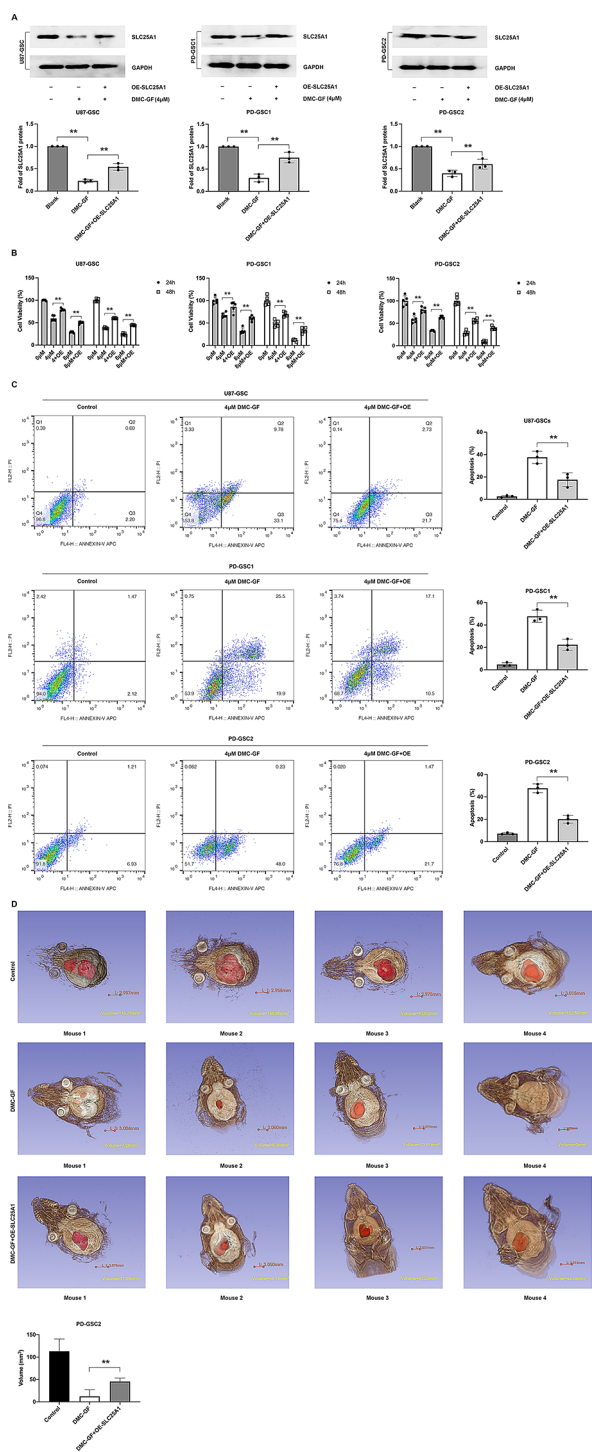


Fig. 6 Effects of SLC25A1 on cell proliferation of GSCs treated with DMC-GF. **(A)** Western blot analysis confirming shRNA-mediated knockdown of SLC25A1 in GSCs ($n=3$). **(B)** CCK-8 analysis of the proliferation rates of GSCs following SLC25A1 knockdown ($n=5$). **(C)** Flow cytometry assays of the apoptosis rates in GSCs with SLC25A1 knockdown ($n=3$). **(D)** Immunohistochemical analysis of the proportion of Ki67-positive cells in the SLC25A1 shRNA transplanted tumours. Three independent biological replicates were included for **(A)**, **(C)** and **(D)**. **, $P<0.01$

and its remarkable blood-brain barrier (BBB) penetration, surpassing that of DMC-BH, was demonstrated, thereby ensuring efficient translocation into the brain. The increased brain-to-blood ratio of DMC-GF indicates enhanced intracranial molecular concentration, providing a robust foundation for further advancements in research. Furthermore, our *in vitro* investigations revealed that DMC-GF exhibited superior anti-glioma



stem cell (GSC) activity and enhanced stability compared to DMC-BH.

We conducted further examinations to unravel the underlying mechanisms of DMC-GF's anti-GSC activity. Our findings compellingly demonstrated that DMC-GF effectively induced dose-dependent apoptosis in GSCs, as evidenced by flow cytometric analysis and TUNEL assay. Notably, Western blot analysis unveiled alterations in crucial apoptotic pathway proteins, with an increase in pro-apoptotic proteins (Bax, Bad, and cleaved-Caspase-3) and a decrease in anti-apoptotic proteins (Bcl-2 and Bcl-xL) upon DMC-GF treatment [21, 22]. Hence, it is plausible that DMC-GF induces apoptosis in GSCs by modulating apoptotic proteins.

To gain deeper insights into the potential targets and mechanisms of action of DMC-GF, we employed mRNA-seq analysis on DMC-GF-treated GSCs. Our pathway analysis revealed significant enrichment in Glycosaminoglycan biosynthesis, MAPK signaling pathway, and Oxidative phosphorylation. Remarkably, DMC-GF was found to exert an impact on mitochondrial function and cellular energy metabolism, as evidenced by its influence on mitochondrial membrane potential and respiratory function [23, 24]. These observations strongly suggest that DMC-GF may interfere with mitochondrial oxidative phosphorylation, implicating its involvement in cellular energy metabolism [25].

Although aerobic glycolysis (the Warburg effect) has long been recognized as a hallmark of cancer metabolism, including GBM, emerging evidence indicates that specific glioma stem cell populations heavily depend on OXPHOS to sustain their energy needs. This metabolic flexibility can endow GSCs with heightened resistance to conventional treatments, as they can switch between glycolysis and OXPHOS to adapt to different microenvironmental conditions [26–28]. By disrupting OXPHOS, DMC-GF not only reduces ATP production but may also alter reactive oxygen species (ROS) levels, thereby affecting intracellular signaling pathways that govern tumour proliferation and survival. These findings underscore that targeting OXPHOS could be a viable therapeutic strategy to overcome the adaptive resistance inherent in GSCs. Future studies should investigate whether DMC-GF exerts synergistic effects when combined with other metabolic modulators or standard GBM therapies, aiming to improve long-term treatment outcomes.

Additionally, we investigated the expression of SLC25A1, a pivotal protein involved in mitochondrial function [29], in glioma tissue and its correlation with patient prognosis. Intriguingly, we observed a substantial upregulation of SLC25A1 expression in glioma tissue compared to normal tissue, and elevated SLC25A1 expression was associated with shorter survival time in glioblastoma patients. Complementing these findings,

our subsequent experiments confirmed heightened SLC25A1 protein levels in tumour tissues relative to normal tissues, thus reinforcing the clinical relevance of SLC25A1 in glioma.

Moreover, we probed the effects of DMC-GF on SLC25A1 expression in GSCs and xenografts. Our results demonstrated that DMC-GF treatment led to a reduction in SLC25A1 expression in GSCs, consistent with the diminished expression observed in xenograft tumour samples. Importantly, these effects were independent of mRNA expression changes, hinting at a potential role of DMC-GF in modulating SLC25A1 protein degradation. Further investigations utilizing a proteasome inhibitor revealed that DMC-GF diminishes SLC25A1 expression through a proteasome-dependent mechanism.

Interestingly, we identified TRIM33 as a potential mediator of DMC-GF-induced SLC25A1 degradation. TRIM33 (also known as TIF1 γ) is a member of the tripartite motif (TRIM) protein family and is involved in various cellular processes, including gene regulation and development [30]. Suppression of TRIM33 expression attenuated the degradation effect of DMC-GF on SLC25A1, implying a dependency on TRIM33. Additionally, inhibition of TRIM33 fostered the growth of orthotopically transplanted tumours, increased the expression of the proliferative marker KI67, and coincided with elevated levels of SLC25A1.

Despite the promising findings presented in this work, several limitations should be noted. First, our experiments focused primarily on a limited range of GSC lines, which may not fully represent the heterogeneity of glioblastoma in clinical settings. Second, although we demonstrated DMC-GF's efficacy *in vitro* and in pre-clinical models, large-scale studies and more extensive *in vivo* validation are needed to confirm translational potential. Third, we employed a single dosing regimen for DMC-GF; further optimization of dose and schedule could refine therapeutic efficacy. Fourth, our *in vivo* experiments had relatively short follow-up periods and did not include intermediate time points, limiting our ability to draw firm causal inferences about tumour progression and therapeutic response over time. Finally, the follow-up periods in our *in vivo* models were relatively short, and longer-term investigations are required to determine whether the observed therapeutic benefits persist over time. Addressing these limitations in future research will strengthen our findings' clinical relevance and robustness.

In summary, our study provides valuable insights into the potential of DMC-GF as a therapeutic agent for glioma treatment. DMC-GF exhibited superior anti-GSC activity and improved metabolic stability compared to its precursor, DMC-BH. Mechanistically, DMC-GF induces apoptosis in GSCs by modulating apoptotic proteins and

influences cellular energy metabolism by interfering with mitochondrial function. Moreover, the clinical relevance of SLC25A1 in glioma was underscored, and TRIM33 emerged as a potential mediator of DMC-GF-induced SLC25A1 degradation.

Abbreviations

GSCs	Glioma stem cells
GLUT1	Glucose transporter protein 1
KEGG	Kyoto Encyclopedia of Genes and Genomes
GBM	Glioblastoma multiforme
TMZ	Temozolomide
GICs	Glioma-initiating cells
BBB	Blood-brain barrier

Supplementary Information

The online version contains supplementary material available at <https://doi.org/10.1186/s12967-025-06355-z>.

Supplementary Material 1

Supplementary Material 2

Supplementary Material 3

Supplementary Material 4

Author contributions

Guan Sun: designed the research study. Lei Shi: Writing– review & editing, Conceptualization. Jian Huang: Writing– review & editing. Xifeng Fei: Methodology, Investigation, Formal analysis, Conceptualization. Bao He: Data curation, Writing– review & editing. Zhixiang Sun: Formal analysis, Investigation, Writing– review & editing.

Funding

This work was supported by the National Natural Science Foundation of China (82273472), Suzhou Key Laboratory of Neuro-Oncology and Nano-Bionics, Suzhou Medical and Health Innovation Project (SKYD2022002), Suzhou Health Key Medical Talent Training Project (GSWS2020112), Jiangsu Provincial Health Commission key project (K2023044), Jiangsu Province 333 Project High level Talents Project (2022360), Jiangsu Province's Natural Science Foundation (BK20211115), Yancheng key research and development plan social development project (YCBE202317), China Postdoctoral Research Funding Program (2019M661906) and China Foreign Experts Project Program.

Data availability

The authors confirm that the data supporting the findings of this study are available within the article.

Declarations

Ethical approval

Approval of the research protocol by an Institutional Reviewer Board: This study has been approved by the Ethics Committee of Affiliated Kunshan Hospital of Jiangsu University (2021-06-004-H01).

Declaration of generative ai and ai-assisted technologies in the writing process

During the preparation of this work the authors used Chatgpt in order to proceed language modification. After using this tool, the authors reviewed and edited the content as needed and take full responsibility for the content of the publication.

Conflict of interest

The authors have no conflict of interest to disclosure.

Received: 21 October 2024 / Accepted: 8 March 2025

Published online: 24 March 2025

References

1. Szklener K, et al. New directions in the therapy of glioblastoma. *Cancers* (Basel). 2022;14(21):5377.
2. Wang J, et al. Progress in the application of molecular biomarkers in gliomas. *Biochem Biophys Res Commun*. 2015;465(1):1–4.
3. Wu W, Daldrup-Link HE, et al. Glioblastoma multiforme (GBM): an overview of current therapies and mechanisms of resistance. *Pharmacol Res*. 2021;171:105780.
4. Gimple RC, et al. Glioblastoma stem cells: lessons from the tumour hierarchy in a lethal cancer. *Genes Dev*. 2019;33(11–12):591–609.
5. Liu J, et al. ZNF117 regulates glioblastoma stem cell differentiation towards oligodendroglial lineage. *Nat Commun*. 2022;13(1):2196.
6. Shi L, et al. Demethoxycurcumin analogue DMC-BH inhibits orthotopic growth of glioma stem cells by targeting JNK/ERK signaling. *Aging*. 2020;12(14):14718–35.
7. Zhou X, et al. Brain penetrating peptides and peptide-drug conjugates to overcome the blood-brain barrier and target CNS diseases. *Wiley Interdiscip Rev Nanomed Nanobiotechnol*. 2021;13(4):e1695.
8. Bergmann S, et al. Blood-brain-barrier organoids for investigating the permeability of CNS therapeutics. *Nat Protoc*. 2018;13(12):2827–43.
9. Tang W, et al. Emerging blood-brain-barrier-crossing nanotechnology for brain cancer theranostics. *Chem Soc Rev*. 2019;48(11):2967–3014.
10. Koch H, et al. The glucose transporter type 1 (Glut1) syndromes. *Epilepsy Behav*. 2019;91:90–3.
11. Han L, et al. Evolution of blood-brain barrier in brain diseases and related systemic nanoscale brain-targeting drug delivery strategies. *Acta Pharm Sin B*. 2021;11(8):2306–25.
12. Wang H, et al. Nanodisk-based glioma-targeted drug delivery enabled by a stable glycopeptide. *J Control Release*. 2018;284:26–38.
13. Shi L, et al. Demethoxycurcumin analogue DMC-BH exhibits potent anticancer effects on orthotopic glioblastomas. *Aging*. 2020;12(23):23795–807.
14. Azari H, et al. Isolation and expansion of the adult mouse neural stem cells using the neurosphere assay. *J Vis Exp*. 2010; 45:2393.
15. Ludwig K, et al. Molecular markers in glioma. *J Neurooncol*. 2017;134(3):505–12.
16. Zhang M, et al. Nestin and CD133: valuable stem cell-specific markers for determining clinical outcome of glioma patients. *J Exp Clin Cancer Res*. 2008;27(1):85.
17. Klotjová I, et al. Encapsulation: A strategy to deliver therapeutics and bioactive compounds?? *Pharmaceuticals* (Basel). 2023;16(3):362.
18. Nolfi-Donagan D, et al. Mitochondrial electron transport chain: oxidative phosphorylation, oxidant production, and methods of measurement. *Redox Biol*. 2020;37:101674.
19. Rosario FJ, et al. Mechanistic target of Rapamycin complex 1 promotes the expression of genes encoding electron transport chain proteins and stimulates oxidative phosphorylation in primary human trophoblast cells by regulating mitochondrial biogenesis. *Sci Rep*. 2019;9(1):246.
20. Hlouschek J, et al. The mitochondrial citrate carrier (SLC25A1) sustains redox homeostasis and mitochondrial metabolism supporting radioresistance of cancer cells with tolerance to cycling severe hypoxia. *Front Oncol*. 2018;8:170.
21. Ye D, et al. Anti-PANoptosis is involved in neuroprotective effects of melatonin in acute ocular hypertension model. *J Pineal Res*. 2022;73(4):e12828.
22. Zhang Y, et al. Notoginsenoside R1 attenuates sevoflurane-induced neurotoxicity. *Transl Neurosci*. 2020;11(1):215–26.
23. Sakamuru S, et al. Mitochondrial membrane potential assay. *Methods Mol Biol*. 2016;1473:17–22.
24. Xu Y, et al. Effects of PKCε knockdown on mitochondrial membrane potential of human glioma cells in vitro and growth of U251 cell-derived tumours in vivo. *Biotech Histochem*. 2023;98(7):501–7.
25. Ashton TM, et al. Higgins, oxidative phosphorylation as an emerging target in cancer therapy. *Clin Cancer Res*. 2018;24(11):2482–90.
26. Nguyen TTT, et al. HDAC inhibitors elicit metabolic reprogramming by targeting super-enhancers in glioblastoma models. *J Clin Invest*. 2020;130(7):3699–716.
27. Vashishta M, et al. Enhanced Glycolysis confers resistance against photon but not carbon ion irradiation in human glioma cell lines. *Cancer Manag Res*. 2023;15:1–16.
28. Duan K, et al. Lactic acid induces lactate transport and Glycolysis/OXPHOS interconversion in glioblastoma. *Biochem Biophys Res Commun*. 2018;503(2):888–94.

29. Tan M, Avantaggiati, et al. Inhibition of the mitochondrial citrate carrier, Slc25a1, reverts steatosis, glucose intolerance, and inflammation in preclinical models of NAFLD/NASH. *Cell Death Differ.* 2020;27(7):2143–57.
30. Verma BK, et al. Regulation of β -catenin by IGFBP2 and its cytoplasmic actions in glioma. *J Neurooncol.* 2020;149(2):209–17.

Publisher's note

Springer Nature remains neutral with regard to jurisdictional claims in published maps and institutional affiliations.